CLINICAL AND EXPERIMENTAL VACCINE RESEARCH

Clin Exp Vaccine Res 2024;13:132-145
https://doi.org/10.7774/cevr.2024.13.2.132
pISSN 2287-3651 • eISSN 2287-366X

Inferring B-cell derived T-cell receptor induced multi-epitope-based vaccine candidate against enterovirus 71: a reverse vaccinology approach

Subrat Kumar Swain[1,*], Subhasmita Panda[2,*], Basanta Pravas Sahu[3,4], Soumya Ranjan Mahapatra[5], Jyotirmayee Dey[5], Rachita Sarangi[2], Namrata Misra[5,6]

Departments of [1]Medical Research and [2]Pediatrics, IMS and SUM Hospital, Siksha "O" Anusandhan Deemed to be University, Bhubaneswar, India; [3]School of Biological Science, The University of Hong Kong, Hong Kong; [4]Decipline of Biosciences and Biomedical Engineering, Indian Institute of Technology, Indore; [5]School of Biotechnology and [6]KIIT-Technology Business Incubator (KIIT-TBI), Kalinga Institute of Industrial Technology (KIIT), Deemed to be University, Bhubaneswar, India

Received: August 26, 2023
Accepted: March 30, 2024

Corresponding author: Rachita Sarangi, MD
Department of Pediatrics, IMS & SUM Hospital, Bhubaneswar, Pin-751003, India
Tel: +91-9437197816, Fax: +91-0674-2386281
E-mail: rachitapaedia@gmail.com; rachitasarangi@soa.ac.in

*These authors contributed equally to this work as the first authors.

No potential conflict of interest relevant to this article was reported.

We are thankful to Indian Council of Medical Research (ICMR) for providing the ICMR-RA fellowship (5/3/8/51/ITR-F/2020). Also, the authors are very much thankful to Medical Research Laboratory of Siksha "O" Anusandhan (deemed to be) University for providing laboratory facility.

Purpose: Enterovirus 71, a pathogen that causes hand-foot and mouth disease (HFMD) is currently regarded as an increasing neurotropic virus in Asia and can cause severe complications in pediatric patients with blister-like sores or rashes on the hand, feet, and mouth. Notwithstanding the significant burden of the disease, no authorized vaccine is available. Previously identified attenuated and inactivated vaccines are worthless over time owing to changes in the viral genome.

Materials and Methods: A novel vaccine construct using B-cell derived T-cell epitopes from the virulent polyprotein found the induction of possible immune response. In order to boost the immune system, a beta-defensin 1 preproprotein adjuvant with EAAAK linker was added at the N-terminal end of the vaccine sequence.

Results: The immunogenicity of the designed, refined, and verified prospective three-dimensional-structure of the multi-epitope vaccine was found to be quite high, exhibiting non-allergenic and antigenic properties. The vaccine candidates bound to toll-like receptor 3 in a molecular docking analysis, and the efficacy of the potential vaccine to generate a strong immune response was assessed through *in silico* immunological simulation.

Conclusion: Computational analysis has shown that the proposed multi-epitope vaccine is possibly safe for use in humans and can elicit an immune response.

Keywords: Reverse vaccinology, Enterovirus 71, Ligand-receptor docking, Immune simulation

Introduction

Rapid *in silico* informatics-based technique vaccinomics has acquired significant attention with the recent back-through in the sequencing of various pathogen genomes and protein sequence databases [1], as it integrates immunogenetics and immunogenomics with bioinformatics for the production of vaccines [2]. The 'vaccinomics' approach has already been used effectively in the combat against disorders like multiple sclerosis, malaria, and tumors [3-5]. Most investigations on the epidemiology, pathophysiology, and vaccine development for hand-foot and mouth disease (HFMD) focus on Enterovirus 71 (EV71) [6]. Serotypes A–F were attributed to EV71 based on the phylogeny of VP1; while serotypes B and C are found all around the world, serotypes D, E, and F are only found in India and Africa [7]. The evolution of EV71 strains makes it difficult to develop a vaccine that is effective against all known strains and subtypes [8]. When constructing an EV71 vaccine candidate, it is crucial to choose a strain that can

protect against the vast majority of different EV71 genotypes and sub-genotypes that are currently available [9].

Currently no vaccine available to prevent HFMD that has been authorized by the US Food and Drug Administration. As HFMD has progressed into a potentially epidemic, there is a pressing need for a vaccine against EV71 to be developed [10]. Numerous major histocompatibility complex (MHC)-restricted epitopes are used to create multi-epitope vaccination, which are then recognized by T-cell receptors (TCR) of multiple clones originating from different T-cell subsets, cytotoxic T lymphocyte (CTL), T helper (Th)- and B-cell epitopes inducing strong cellular and humoral immune responses simultaneously produce sustained immune responses and lower the risk of aberrant immunological reactions or adverse consequences caused by noxious substances [11,12].

Materials and Methods

Selection of EV strain and extraction of protein sequences

The whole genome sequence of enterovirus A71 strain along with whole proteome, the National Center for Biotechnology Information (NCBI) database was searched for all encoded proteins. The polyprotein that plays crucial role in viral pathogenesis were chosen for vaccine candidate development, and their FASTA-formatted sequences were obtained from the UniProt database (https://www.uniprot.org/).

Forecasting and assessment of epitopes

NetCTL 1.2 server (https://services.healthtech.dtu.dk/services/NetCTL-1.2/) was used to screen the antigenic CTL epitope adjusting threshold 0.05, 0.15, and 0.75 for MHC-I binding affinity [13]. Immune Epitope Database (IEDB) MHC-I binding resource selected all strong binding epitopes with half maximal inhibitory concentration (IC50) <500. Protein sequences were submitted to the NetMHCII Pan 3.1 server (https://services.healthtech.dtu.dk/services/NetMHCIIpan-3.2/) [14] and confirmed from IEDB research resource to predict MHC class II restricted helper T lymphocyte (HTL) epitopes. ABCPred2.0 (http://crdd.osdd.net/raghava/abcpred/) is used to predict the linear B-cell epitopes [15]. AllerTop ver. 2.0 (https://www.ddg-pharmfac.net/AllerTOP/) measured the construct's allergenicity [16], while the VaxiJen online server (https://www.ddg-pharmfac.net/vaxijen/VaxiJen/VaxiJen.html) predicted the vaccine's antigenicity [17]. When the protein construct was overexpressed in *Escherichia coli*, the SOLpro online tool (http://scratch.proteomics.ics.uci.edu/) estimated solubility [18]. Finally, the ToxinPred server (http://crdd.osdd.net/raghava/toxinpred/) tested all epitopes for toxicity [19]. All selected epitopes are nontoxic, antigenic, and nonallergenic and should induce immune receptors.

Conservancy analysis and population coverage analysis

IEDB was used to determine the degree of epitope dissemination in the homologous protein set and the conservancy of selected B cell, CTL, and HTL epitopes [20]. Vaccine candidates should protect global populations. IEDB's population coverage tool was used to determine the predicted T-cell epitopes' population coverage [21].

Construction of muti-epitope vaccine candidate and property analysis

The efficacy of the vaccine is enhanced when one adjuvant is added at the N-terminal end, i.e., beta-defensin 1 preproprotein. EAAAK, KK, AAY, and GPGPG act as a linker to connect the B-cell epitope, CTL, and HTL, respectively. The ExPASy ProtParam online web tool (https://web.expasy.org/protparam/) was used to assess the physicochemical parameters of the final vaccine construct, including amino acid composition, theoretical PI, molecular weight, instability index, half-life, aliphatic index, and grade average of hydropathicity (GRAVY) [22]. To predict the vaccine candidate as antigen, non-allergen, and non-toxic, VaxiJen ver. 2.0, AllerTop, and ToxinPred servers were used.

Structure prediction and refinement

The secondary structure of multi-epitope vaccine construct was generated by online tool PSIPRED (https://bio.tools/psipred) [23]. The tertiary structure was constructed using Robetta server (https://robetta.bakerlab.org/). The modelled structure was refined by GalaxyRefine server (https://galaxy.seoklab.org/cgi-bin/submit.cgi?type=REFINE) [24]. Using the PROCHECK server (https://www.ebi.ac.uk/thornton-srv/software/PROCHECK/), a Ramachandran plot was generated that illustrates the energetically allowed and disallowed angles psi (ψ) and phi (φ) of amino acids [25]. The server isolates the plots for glycine and proline residues and applies the PROCHECK concept to validate the protein structure, using the Ramachandran plot. SAVES server (https://saves.mbi.ucla.edu/) was used for the assessment of vaccine construct.

Disulfide bond engineering for vaccine stability

Whilst also changing cysteine residues in a highly mobile re-

gion of the protein, disulfide engineering can generate new disulfide bridges in the target protein. It significantly strengthens the geometric shape of the protein and are therefore essential for stability. Disulfide by Design v2.0 (http://cptweb.cpt.wayne.edu/DbD2/) was used to engineer the disulfide bond, which searches for pairs of amino acid residues where cysteine can replace the original amino acid [26].

Discontinuous B-cell epitopes

Prediction of discontinuous B-cell epitopes of the vaccine design were performed using Ellipro tool on the IEDB server (http://tools.iedb.org/ellipro/) [20]. Discontinuous epitopes are grouped together based on their distance R, denoted in Å, with a higher discontinuous epitope having a grater R value.

Molecular docking of final vaccine candidate with immune receptor

Molecular docking is a computer base method in which a ligand and a receptor interact to form a stable aggregate with a determined score indicating the degree of binding interaction [27]. Toll-like receptor 3 (TLR3) (PDB ID:1ziw) was used as a receptor and the refined vaccine construct was used as the ligand. ClusPro online server (https://cluspro.org/login.php) was used to predict the interaction between the protein molecules.

Molecular dynamic simulation

GROMACS 2019 package (https://manual.gromacs.org/documentation/2019/index.html) and OPLS-e force field (Schrödinger Inc., New York, NY, USA) were used to do the MD simulation. The TIP3P water model (https://docs.lammps.org/Howto_tip3p.html) was utilized in order to solvate the protein complex. Then, a neutral physiological salt concentration was achieved by adding sodium and chloride ions. Until a Fmax value of less than 10 kJ/mol was determined, the energy of the system was minimized using the steepest descent algorithm. The Linear Constraint Solver technique was used to impose constraints on all of the covalent bonds, ensuring that their lengths remained fixed throughout the simulation. The Particle Mesh Ewald approach was used to account for the long-range electrostatic interactions, and 0.9 nm was chosen as the threshold radius for the Coulomb and Van der Waals short-range interactions. In the next step, equilibrations were carried out for each system at 100 ps NVT (constant number of particles [N], volume [V], and temperature [T]) and 100 ps NPT (constant number of particles [N], pressure [P], and temperature [T]). Then, GROMACS modules were used to do the necessary analysis, and xmgrace was used to generate the necessary charts and figures from the 50 ns of simulations run under periodic boundary conditions.

A5V codon adaptation, expression, and purification

Codon optimization was used to increase expression of the recombinant protein. In order to assess the quantities of protein production in *E. coli* (strain k12), the JAVA codon adaptation tool (https://www.jcat.de/) was used to acquire the codon adaptation index (CAI) values and GC content. Multi-epitope vaccine gene sequence optimization resulted in cloning into the *E. coli* plasmid vector pET28a (+). The sequence has been modified to include restriction sites at both the N and C termini, specifically for the enzymes EcoRI and BamHI. Snapgene software (https://www.snapgene.com/) was used to insert the final optimized sequence of the vaccine construct, including the restriction sites, into the plasmid vector pET28a (+).

Immune simulation

C-ImmSim server (https://kraken.iac.rm.cnr.it/C-IMMSIM/index.php) was used to analyze the immune response of the vaccine construct, following cloning an *in silico* immune simulation was conducted. Three key elements of a functioning mammalian system (the lymph node, bone marrow, and thymus) are simulated simultaneously. In real life, it is advised to wait for 4 weeks between vaccination doses [28]. The interval between vaccine doses 1 and 2 should be at least 4 weeks. To simulate 1,050 simulation steps, all primary parameters of the C-ImmSim server were set to default, and three injections containing 1,000 vaccine proteins were given 4 weeks with time 1 hour, 8 hours, and 168 hours for the first, second, and third injections, respectively (each time step equals to 8 hours in real life, and time-step 1 is injection at time=0).

Results

Analysis of retrieved protein sequence and profiling

In order to predict the B- and T-cell epitopes and design a multi-epitope-based vaccine, the whole genome sequence of EV71 (under the accession number: AAB39968.1) was obtained from the NCBI database. The NCBI database revealed that human beta-defensin 1 (accession number: NP 005209.1) is an adjuvant that may stimulate an immune response against viruses. According to ExPASy Protparam's analysis of the EV71 polyprotein's physicochemical properties, the protein is stable with an instability index of 36.05, an aliphatic index of 83.15,

 https://doi.org/10.7774/cevr.2024.13.2.132

and a GRAVY score of -0.198. VaxiJen ver. 2.0 and AllerTop ver. 2.0 were used to make the antigenicity and allergenicity predictions, respectively with an antigenicity score of 0.5017. Fig. 1 illustration the schematic representation of the complete process.

CTL, HTL, and B-cell epitope prediction

Using the NetCTL ver. 2.0 server, we were able to predict 9-mer CTL epitopes from EV71. Finally, these potential epitopes were screened using IC50 values below 500. Table 1 lists the five antigenic and non-allergenic potential epitopes. Both the innate and adaptive immune systems rely heavily on interferon-γ (IFN-γ), a cytokine that has been shown to have antiviral, immunological regulatory, and anticancer effects. The IFN epitope server identified sequences capable of triggering IFN-γ. The viral polyprotein was used to predict 29 non-allergenic, antigenic, and non-toxic HTL epitopes (15-mer). Out of them, only nine were determined to have IFN-γ positive epitopes. Dual human allele epitopes with no overlap HLA-DRB1*04:01, HLA-DRB1*13:02, HLA-DRB1*08:02, HLA-DRB3*02:02, HLA DRB1*07:01, HLA-DRB1*01:01, HLA-DRB1*04:05, HLA-DRB1*11:01, and HLA-DRB1*09:01 were chosen as they have the IC50 values of the chosen epitopes were lower than 100. Table 2 demonstrates that all verified epitopes are non-allergenic and non-toxic antigens. ABCPred was able to accurately predict the B-cell epitope for the multi-epitope vaccination with an accuracy of 65.93%.

Designing of a multi-epitope vaccine construct

To design a novel vaccine with binding affinity, antigenicity, non-toxicity, and non-allergenicity, two B-cell, five CTL, and two HTL epitopes were nominated. Human-defensin 1 was

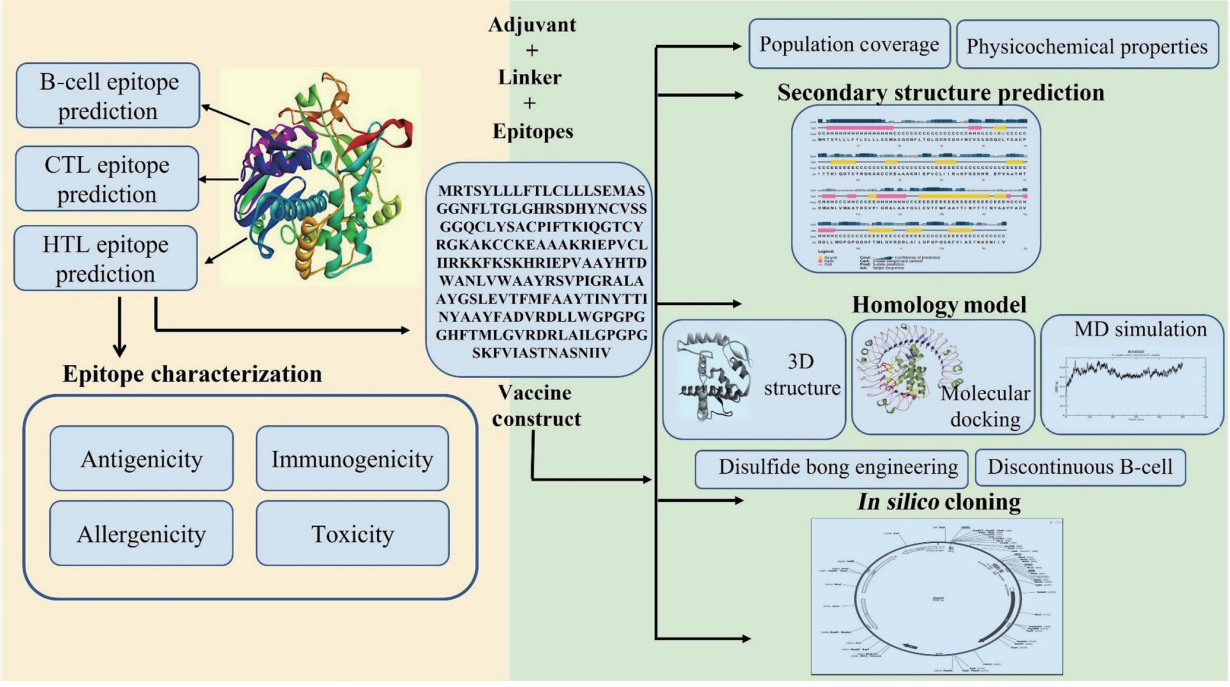

Fig. 1. Flow chart showing the structural arrangement of designed vaccine. CTL, cytotoxic T lymphocyte; HTL, helper T lymphocyte; 3D, three-dimensional; MD, molecular dynamics.

Table 1. Prediction of CTL epitopes for multi-epitope-based vaccine development

CTL peptide seq.	Allele	Start-end	IC50	Antigenicity	Allergenicity	Immunogenicity
HTDWANLVW	HLA-B*58:01	887–895	5.37	1.6136	Non-allergen	0.27686
RSVPIGRAL	HLA-B*57:01	2,169–2,177	0.67	1.5002	Non-allergen	0.23028
GSLEVTFMF	HLA-B*58:01	436–444	22.20	1.4707	Non-allergen	0.17009
TINYTTINY	HLA-B*35:01	24–32	80.12	1.2485	Non-allergen	0.17706
FADVRDLLW	HLA-B*58:01	996–1,004	11.93	1.1216	Non-allergen	0.10418

CTL, cytotoxic T lymphocyte; IC50, half maximal inhibitory concentration.

Table 2. Prediction of HTL epitopes for multi-epitope-based vaccine development

HTL epitope sequence	Allele	Antigenicity	Allergenicity	Immunogen	IFN-γ	Conservancy (%)
GHFTMLGVRDRLAIL	HLA-DRB5*01:01	1.57	Non-allergen	0.1912	Positive	100
	HLA-DQA1*01:01					
	HLA-DRB1*01:01					
	HLA-DRB1*04:05					
	HLA-DRB1*11:01					
	HLA-DQA1*01:02/DQB1*06:01					
	HLA-DRB1*07:01					
	HLA-DRB1*09:01					
	HLA-DRB1*15:01					
	HLA-DRB1*03:01					
	HLA-DPA1*03:01/DPB1*04:01					
	HLA-DRB1*12:01					
	HLA-DRB4*01:01					
	HLA-DQA1*05:01/DQB1*02:01					
	HLA-DPA1*01:03/DPB1*02:02					
	HLA-DRB3*01:01					
	HLA-DRB1*08:02					
	HLA-DPA1*02:01/DPB1*05:01					
	HLA-DPA1*01:03/DPB1*04:01					
	HLA-DPA1*02:01/DPB1*14:02					
	HLA-DRB1*13:02					
	HLA-DRB3*02:02					
	HLA-DPA1*02:01/D PB1*01:03					
	HLA-DQA1*04:01/DQB1*04:01					
	HLA-DRB1*04:01					
SKFVIASTNASNIIV	HLA-DRB1*04:01	0.4338	Non-allergen	0.17863	Positive	100
	HLA-DRB3*02:02					
	HLA-DRB1*08:02					
	HLA-DRB1*13:02					
	HLA-DRB1*07:01					
	HLA-DRB1*01:01					
	HLA-DRB1*04:05					
	HLA-DPA1*02:01/DPB1*14:01					
	HLA-DRB3*01:01					
	HLA-DRB1*11:01					
	HLA-DRB1*09:01					
	HLA-DQA1*05:01/DQB1*03:02					
	HLA-DRB5*01:01					
	HLA-DRB4*01:01					
	HLA-DRB1*15:01					
	HLA-DRB1*03:01					
	HLA-DQA1*01:02/DQB1*06:02					
	HLA-DRB1*12:01					
	HLA-DPA1*01:03/DPB1*04:02					
	HLA-DQA1*04:01/DQB1*04:01					
	HLA-DPA1*02:01/DPB1*01:01					
	HLA-DQA1*03:01/DQB1*03:02					
	HLA-DQA1*05:01/DQB1*02:02					

HTL, helper T lymphocyte; IFN-γ, interferon-γ.

 https://doi.org/10.7774/cevr.2024.13.2.132

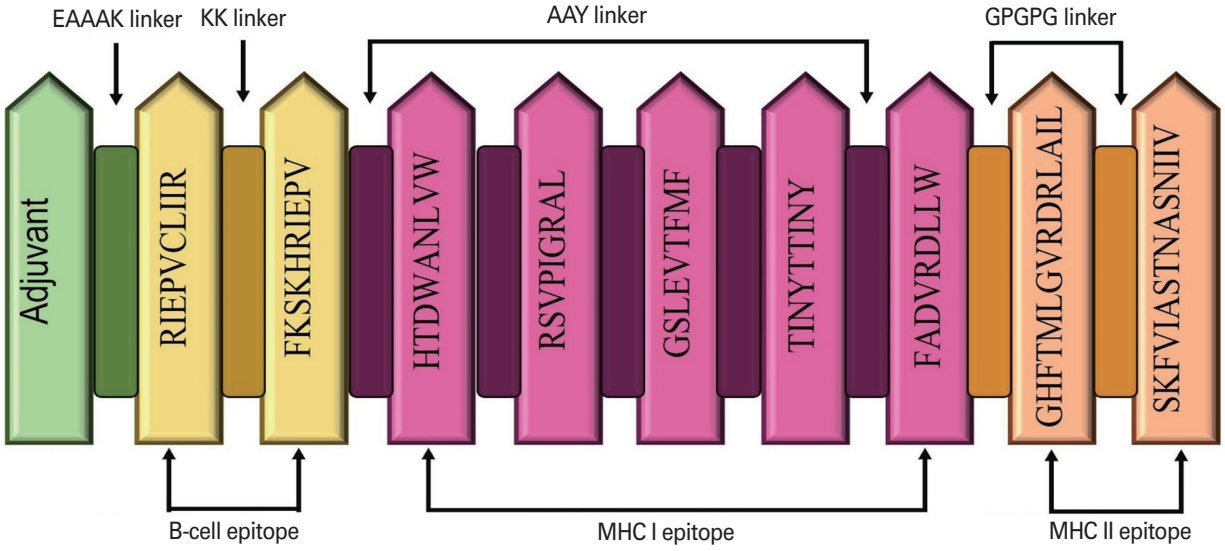

Fig. 2. Schematic representation of the final vaccine construct. The vaccine construct contains 191 amino acids: beta-defensin 1 adjuvant at the N-terminal region following B-cell, cytotoxic T lymphocyte (CTL), and helper T lymphocyte (HTL) epitopes with dissipated linkers EAAAK, KK, AAY, and GPGPG, respectively. MHC, major histocompatibility complex.

added to the N-terminus to boost vaccine efficacy. Four linkers stabilized the construct. EAAAK linked the adjuvant to B-cell epitopes. KK, AAY, and GPGPG linked B-cell, CTL, and HTL epitopes, respectively (Fig. 2). Antigenicity score of 0.828 at 0.4 threshold predicted non-allergenicity of the vaccine design. The vaccine structures have 195 amino acid residues, $C_{967}H_{1504}N_{260}O_{261}S_{12}$. Synthetic vaccinations have 21 kDa molecular weights and 9.40 isoelectric points. Human, yeast, and *E. coli* half-lives are 30, 10, and 10 hours, respectively (10 hours). Protein stability is 31.51. If Gravy is positive, the construct vaccine is polar. The aliphatic index and Gravy value are 90.15 and 0.196 (Table 3). Overexpression of the construct resulted in insolubility, as anticipated by SOLpro (solubility was 0.673).

Table 3. Physicochemical properties of vaccine construct protein

Physicochemical properties	Results
No. of amino acids	195
Molecular weight	21,332.88
Theoretical isoelectric point	9.40
Total no. of negatively charged residues	10
Total no. of positively charged residues	21
Chemical formula	$C_{967}H_{1504}N_{260}O_{261}S_{12}$
Total no. of atoms	3,004
Instability index	31.51
Aliphatic index	90.15
Grand average of hydropathicity	0.196
Solubility upon over expression	Insoluble

Structure analysis, refinement, and validation

Alpha helices accounted for 33.85% of the expected secondary structure, followed by extended strands (25.13%), and random coils (32.31%) (Fig. 3). Robetta, among the top five models, was used to create the major tertiary structure of the vaccine construct, with a higher C score indicating more model confidence. So, the three-dimensional (3D) model was improved further by the GalaxyRefine server, yielding five final models for the vaccine build. Model 1 has the best-refined structure according to a variety of criteria including a global distance test-high accuracy of 0.978, a relative mean square deviation (RMSD) of 0.301, a MolProbity of 2.167, a clash score of 14.6, a bad rotamer of 0.6, and a Rama favored score of 91.7% (Fig. 4). The Ramachandran plot showed that 91.7% of residues were in the preferred area after running the 3D structure through PROCHECK and SWISS-Model. Ramachandran plots show energy-permissible and non-permissible dihedral angles (psi and phi). ERRAT and verify3D score of 84.10% showed that the model driven after GalaxyRefine had better stereochemical quality, validating the quality evaluation (Fig. 5).

Epitope conservancy analysis and population coverage

All the selected epitopes were analyzed using the IEDB conservancy analysis tool across all enterovirus strains. Four antigenic epitopes were 100% conserved across isolates from

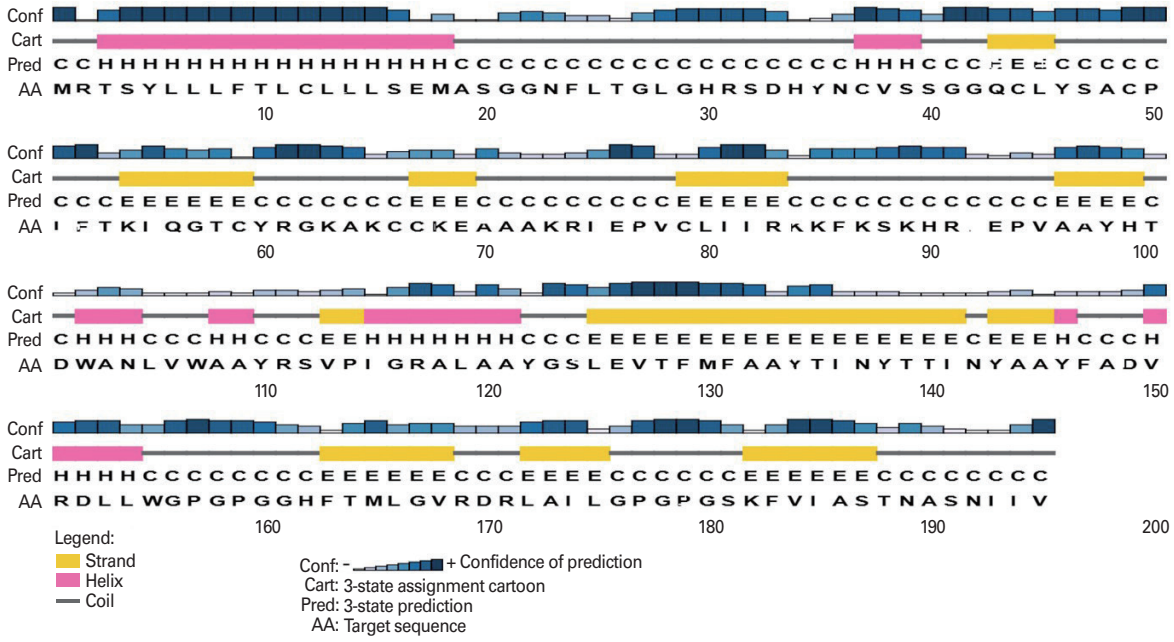

Fig. 3. Secondary structure of the vaccine construct showing alpha helix, beta sheet, and coil-coil region. AA, amino acids.

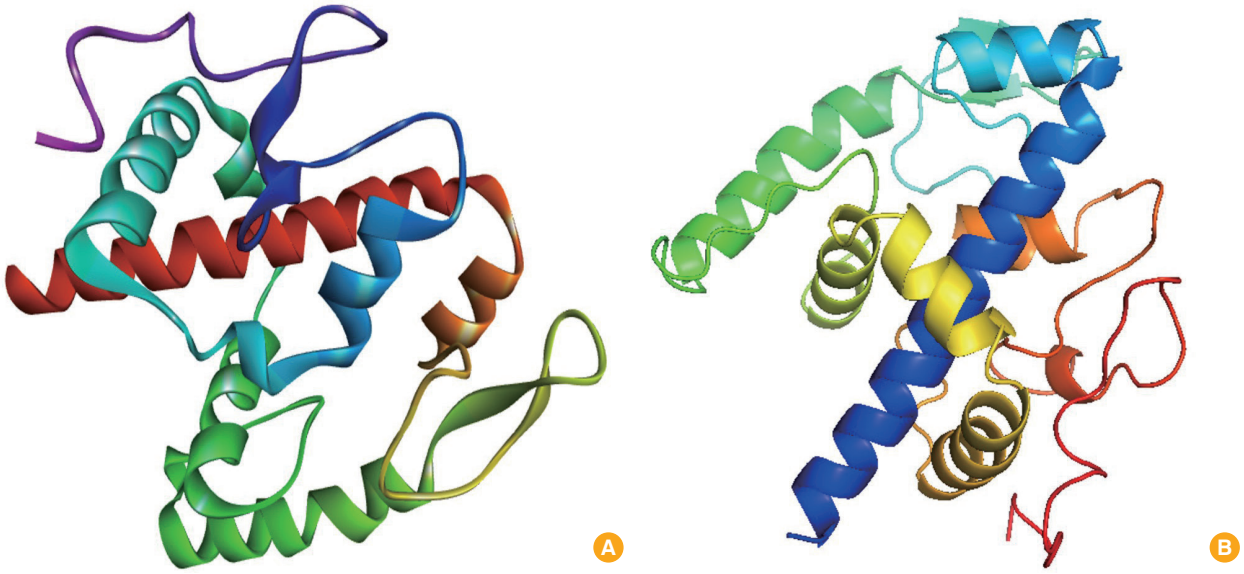

Fig. 4. Structure prediction of vaccine construct. **(A)** Homology modelling of the vaccine. **(B)** Refinement structure of the final vaccine construct.

different nations, while more than 80% were shared. Allelic frequency statistics show that the identified T-cell epitopes are ideal for the candidate protein vaccine due to their worldwide distribution. The predicted epitopes covered 95.6% of the global population in 109 countries across 16 regions. Nearly all nations had coverage above 90%.

Disulfide bond engineering

The analysis showed that for disulfide bond engineering, a total of 124 pairs of residues were explored. Among them, only those pairs of residues fulfilling all the criteria—i.e., where the energy and χ^3 values must be within 2.2 and between -87° to +97°, respectively—were accepted. As a result, only one pair of residues fulfilled all the criteria. Therefore, one mutation was generated on the residue pair ALA48–ASP152, with

 https://doi.org/10.7774/cevr.2024.13.2.132

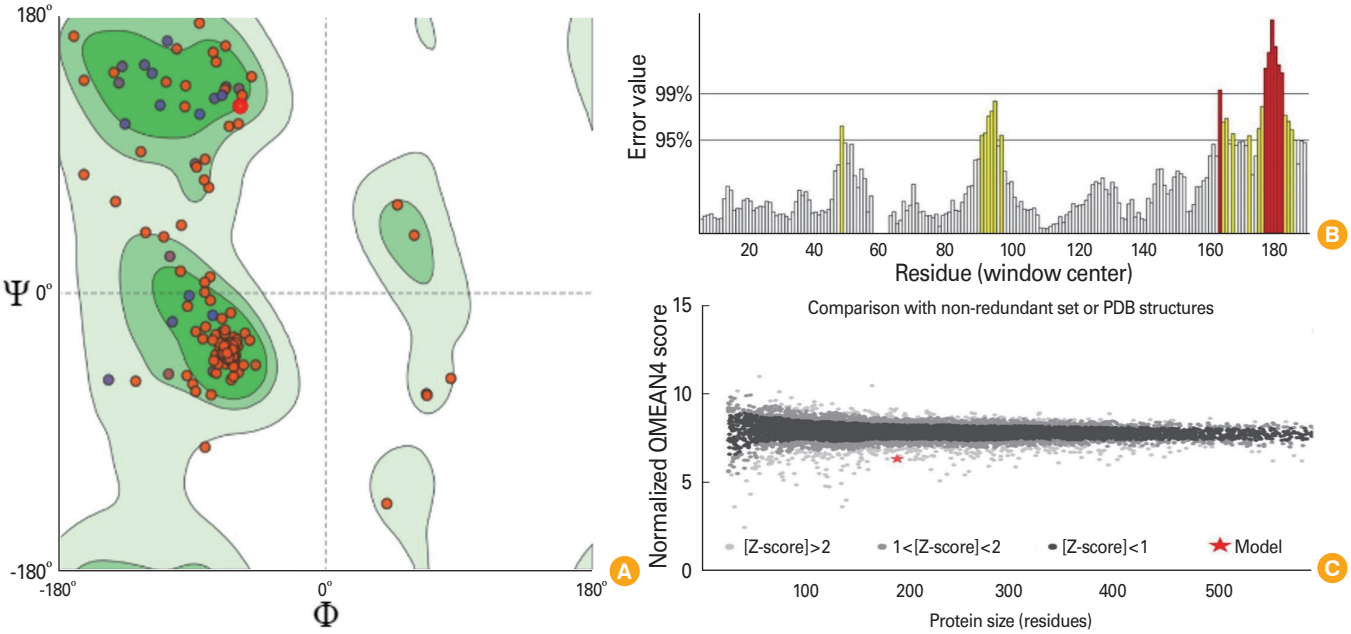

Fig. 5. (A–C) Assessment and validation of final model by SAVES web server (https://saves.mbi.ucla.edu/). Ramachandran plot analysis of refined structure showing amino acid residues in the favored, allowed, and outlier region. QMEAN4, qualitative model energy analysis 4.

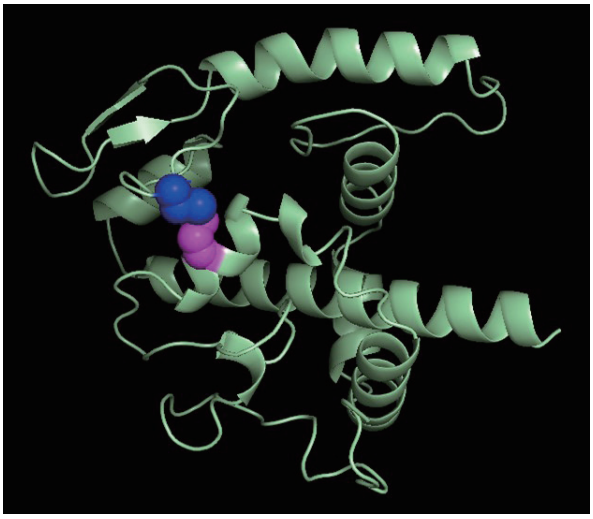

Fig. 6. Disulfide bond engineering of the vaccine construct mutant model showing the disulfide bond formation.

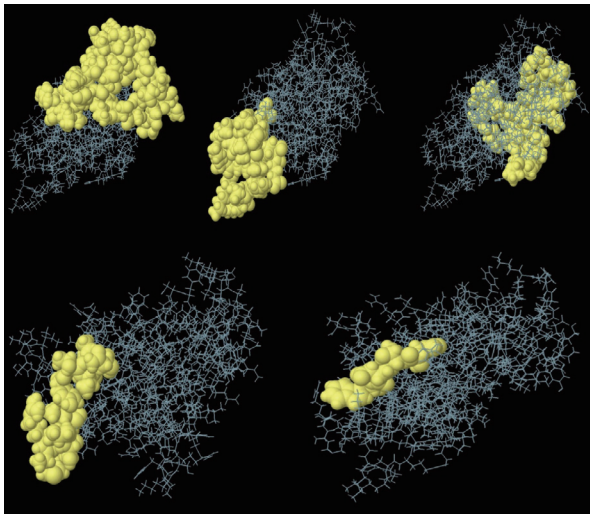

Fig. 7. Predicted confirmational B-cell epitopes by Ellipro tool (http://tools.iedb.org/ellipro/).

Table 4. Confirmational discontinuous B-cell epitope

No.	Residues	No. of residues	Score
1	A:E76, A:P77, A:V78, A:C79, A:L80, A:I81, A:I82, A:R83, A:K84, A:K85, A:F86, A:K87, A:S88, A:K89, A:H90, A:R91, A:I92, A:E93, A:P94, A:Y98	20	0.782
2	A:T26, A:G27, A:G29, A:H30, A:R31, A:S32, A:D33, A:Y35, A:N36, A:S39, A:S40, A:G41, A:G42, A:C44, A:Y46, A:S47, A:A48, A:C49, A:P50, A:F52, A:T53, A:K54, A:I55, A:Q56, A:G57, A:T58, A:C59, A:Y60, A:R61, A:G62, A:K63, A:A64, A:K65, A:C66, A:K68, A:E69, A:A70, A:A72, A:K73, A:R74	40	0.652
3	A:P114, A:G116, A:A122, A:G123, A:S124, A:L125, A:E126, A:V127, A:F129, A:M130, A:Y134, A:N137, A:G156, A:P157, A:G158, A:P159, A:G160, A:G161, A:I174, A:L175, A:G176, A:P177, A:G178, A:P179, A:G180, A:S181, A:K182, A:F183, A:V184, A:I185, A:A186, A:S187, A:T188, A:N189, A:A190, A:S191, A:N192, A:I193, A:I194, A:V195	40	0.645
4	A:M1, A:R2, A:T3, A:S4, A:Y5, A:L6, A:Y138, A:T139, A:T140, A:I141, A:N142	11	0.619
5	A:H99, A:T100, A:D101, A:W102	4	0.508

a χ^3 angle of -67.13 and energy of 1.68, respectively. The disulfide bonds with blue and pink colors are shown in the created mutant (Fig. 6).

Conformational B-cell epitope prediction

Four discontinuous B-cell epitopes contain115 amino acid residues which values are ranging from 0.50–0.78 and the size ranging from 4–40 residues were estimated to be suited in five discontinuous epitopes (Fig. 7). The individual scores were shown in Table 4.

Molecular docking

The immunological response to EV71 is bolstered by toll-like receptor 3 [28]. Therefore, using ClusPro, we docked the final vaccine construct to TLR-3 (PDB ID:1ziw), and the resulting complex had an energy score of -1,183.2 when evaluated in Pymol, making it the best possible candidate for an effective vaccination. Many strong hydrogen bond (H-bond) connections with reduced distance between the interacting residues were seen between the vaccine construct and the immunological receptor, demonstrating high binding affinity. The residues of docked vaccine-TLR3 complex showing H-bond interactions with distance were documented (Table 5, Fig. 8).

Molecular dynamic simulation

MD simulations used the optimal molecular docking complex. After that, a 50-ns MD simulation was run on the complex, and the results were analyzed for RMSD, root mean square fluctuation (RMSF), H-bonds, and radius of gyration

Table 5. Hydrogen bond (distance Å) and interaction of vaccine candidate with TLR3

TLR-3	Vaccine	Distance (Å)
SER38	THR3	1.8
GLU33	LYS85	1.7
GLU33	TRP102	1.9
THR54	ASP101	2.0
SER132	ILE194	1.9
GLN107	ASN137	2.0
GLN107	THR139	1.9
ASN105	THR139	2.0
LYS102	TYR146	1.6
GLU127	ARG169	1.8
ASP153	ARG169	1.9
LYS201	ASP170	1.7
GLU175	ARG171	1.9
LYS200	SER47	1.7

TLR3, toll-like receptor 3.

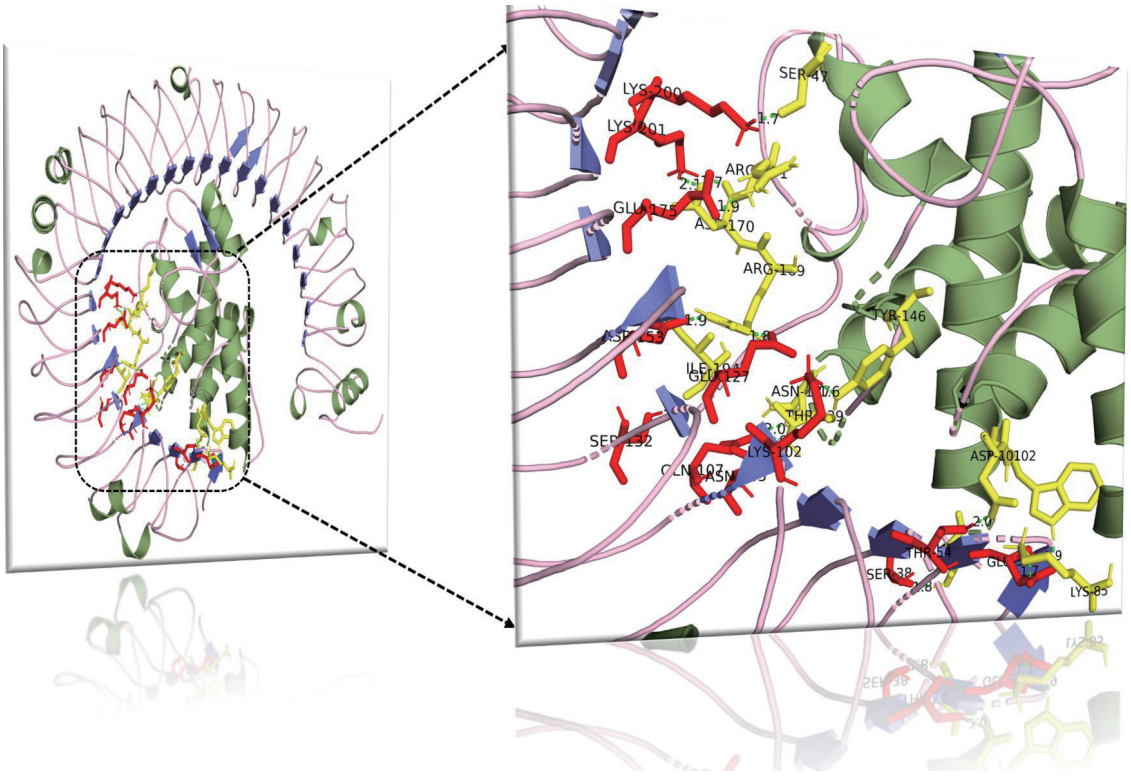

Fig. 8. Molecular docking of final vaccine construct with toll-like receptor 3 complex and hydrogen bond interaction map.

 https://doi.org/10.7774/cevr.2024.13.2.132

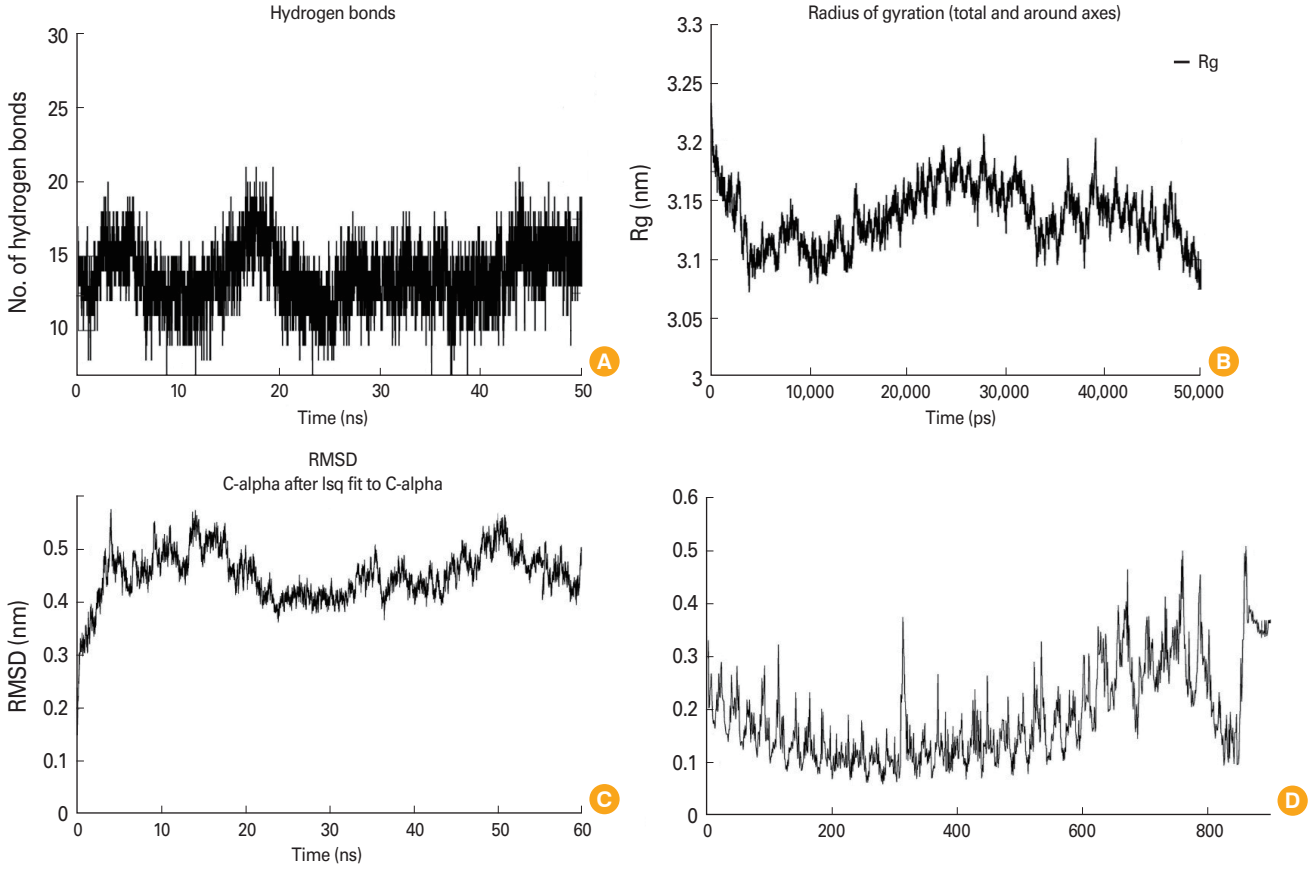

Fig. 9. (A–D) Molecular dynamic simulation showing root mean square deviation (RMSD) and root mean square fluctuation analysis of protein backbone and side chain residues.

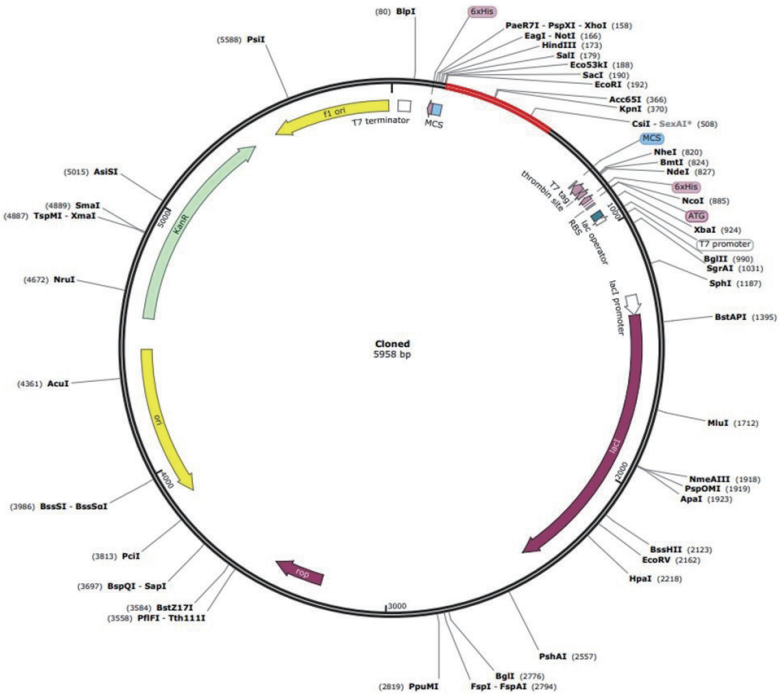

Fig. 10. *In silico* cloning of the gene sequence into the pET28 (+) expression vector. The red part showing the gene coding for multi-epitope vaccine construct and the black region showing the vector backbone.

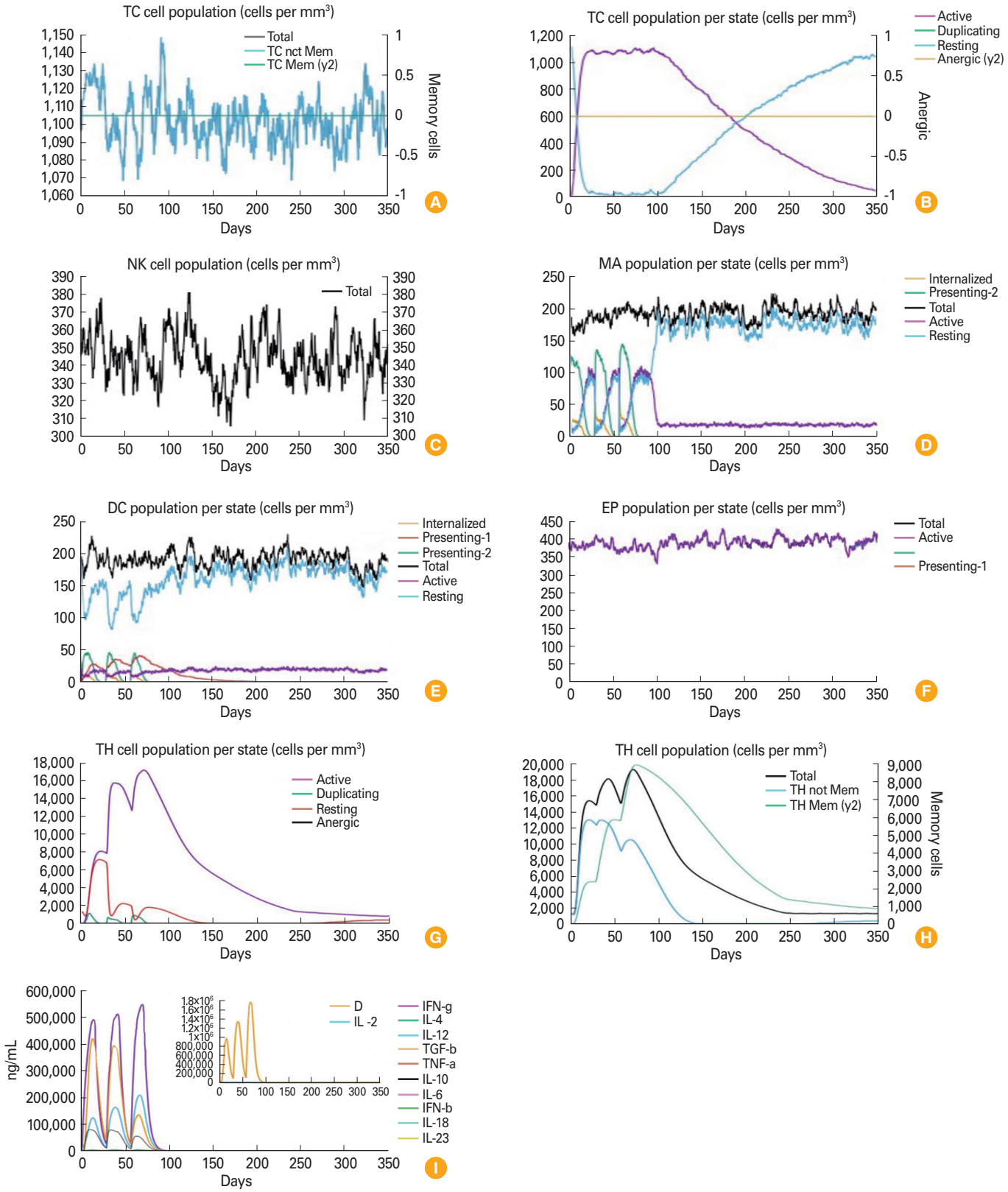

Fig. 11. *In silico* immune simulation by C-ImmSim (https://kraken.iac.rm.cnr.it/C-IMMSIM/index.php) using vaccine as an antigen. **(A)** Cytotoxic T-cell population. **(B)** Cytotoxic T-cell population per state. **(C)** Natural killer cell population. **(D)** Macrophage cells population per state. **(E)** Dendritic cells population per state. **(F)** Epithelial cells population per state. **(G)** Helper T-cell population per state. **(H)** Helper T-cell population. **(I)** Concentration of cytokine and interleukins.

 https://doi.org/10.7774/cevr.2024.13.2.132

(Rg). Considering all atoms, the receptor-vaccine combination's average RMSD was 0.4 nm (Fig. 9). RMSF can reveal a protein's residue-by-residue dynamics relative to its initial state. RMSF analysis of protein atoms revealed residue-level conformational behavior of the ligand-receptor combination. RMSF is 0.3 nm (Fig. 9). The vaccine-receptor complex has an average of 15–18 hydrogen bonds (Fig. 9). The vaccine-TLR-3 complex's Rg is 3.15 nm, according to molecular dynamics simulation (Fig. 9).

Codon optimization and *in silico* cloning

The vaccine design in *E. coli* strain k12 has its codon use optimized using the JAVA codon adaptation tool for maximum expression. Excellent expression of the vaccine candidate in *E. coli* host was predicted thanks to a CAI of 1.0 for the optimized nucleotide sequence and a GC content of 52.30 for the modified sequence. Cloning the vaccine construct will be easier with two restriction endonucleases, such as EcoRI and BamHI, placed at opposite ends of the DNA. The altered codon sequences were then inserted into the plasmid vector pET28a (+) with the aid of SnapGene software, yielding a recombinant plasmid sequence of 5958bp in length (Fig. 10).

Immune simulation

The real immunological response of the produced vaccine in the mammalian system is predicted by the C-ImmSim server. Secondary and tertiary immune responses are characterized by an increase in B-cells and by the production of large amounts of immunoglobulin M (IgM), immunoglobulin G (IgG)1+IgG2, and IgM+IgG despite a reduction in antigen concentration [29]. We observed an upsurge in IFN-g, TGF-b, interleukin (IL)-10, and IL-12 and a reduction in IL-4, IL-6, IL-18, IL-23, TNF-a, and IFN-b. The immune simulation analysis showed that our vaccine candidate can act as a prominent antigen by inducing antibody production. Based on immunological responses, the human immune system recognizes the polyprotein from day 1 and produces antibodies from day 4. IFN-γ production is high from the second day onward and activates macrophages, natural killer (NK) cells, and neutrophils. Our vaccine activates B memory (y2) cells and IgM (Fig. 11). Th-cell formation is crucial to Ig formation. From the 2nd day onward, the Th-memory (y2) cell population increased until it reached 9,000 memory cells per mm^3. Th-cells activated only after day 5 (Fig. 11). NK cell populations fluctuate greatly. Macrophages remained stable. The vaccination increased interferon-γ, TGF-beta, IL-10, and IL-12 production (Fig. 11). The first two vaccinations increased interferon-γ, TGF-beta, IL-12, and IL-10 concentrations. C-IMMSIM simulations predicted the multi-epitope vaccine would activate the immune response.

Discussion

Vaccine development efforts for EV71 have mostly emphasized on inactivated whole-virus vaccines [30], VLP vaccines [31], live attenuated vaccines [32], polypeptide vaccines [33], and DNA vaccines [34]. During the last decade, EV71 has shown a stronger tendency for mutation, and many new genotypes have since emerged and spread over the world [28,35]. Wu et al. [35] tested the immunogenicity of inactivated whole-virus candidates grown in serum-containing and serum-free conditions in microcarriers and adjuvanted with alum [36]. According to the results of Tung et al. [36], analysis of VP1 DNA immunogenicity, the VP1 DNA vaccine candidate might generate serum neutralizing antibodies in a high dose level (100 g) in mice, which may not be practical in humans [37]. While recombinant VP1 and DNA vaccines may be less expensive to produce, inactivated whole-virus vaccines seem to be more immunogenic overall [38]. The immunoinformatics technique has been applied on a worldwide scale to lessen the financial and time requirements typically associated with the development process.

Pathogen genomics and proteomics are revealing new vaccine formulation and development methods [39,40]. Multi-epitope-based vaccinations using immunoinformatics elicit a targeted immune response while preventing reactions to potentially harmful epitope antigens. Immunological simulation assessed vaccine reactions. Proteins must be surface-presented and immune system-recognized to be used in vaccines. This study also shows that combining B-cell and T-cell epitopes to generate a strong and long-lasting immune response is an effective way to establish cellular and humoral immunity.

ORCID

Subrat Kumar Swain *https://orcid.org/0000-0002-9173-1727*
Subhasmita Panda *https://orcid.org/0000-0002-2813-9931*
Basanta Pravas Sahu *https://orcid.org/0000-0002-6454-0976*
Soumya Ranjan Mahapatra *https://orcid.org/0000-0002-8927-458X*
Jyotirmayee Dey *https://orcid.org/0000-0002-5543-7109*
Rachita Sarangi *https://orcid.org/0000-0002-1204-5746*
Namrata Misra *https://orcid.org/0000-0003-1813-6478*

References

1. Poland GA, Ovsyannikova IG, Jacobson RM. Application of pharmacogenomics to vaccines. Pharmacogenomics 2009;10:837-52.
2. Flower DR. Bioinformatics for vaccinology. Hoboken (NJ): John Wiley & Sons; 2008.
3. Bourdette DN, Edmonds E, Smith C, et al. A highly immunogenic trivalent T cell receptor peptide vaccine for multiple sclerosis. Mult Scler 2005;11:552-61.
4. Lopez JA, Weilenman C, Audran R, et al. A synthetic malaria vaccine elicits a potent CD8(+) and CD4(+) T lymphocyte immune response in humans: implications for vaccination strategies. Eur J Immunol 2001;31:1989-98.
5. Knutson KL, Schiffman K, Disis ML. Immunization with a HER-2/neu helper peptide vaccine generates HER-2/neu CD8 T-cell immunity in cancer patients. J Clin Invest 2001; 107:477-84.
6. Xing W, Liao Q, Viboud C, et al. Hand, foot, and mouth disease in China, 2008-12: an epidemiological study. Lancet Infect Dis 2014;14:308-18.
7. Cox JA, Hiscox JA, Solomon T, Ooi MH, Ng LF. Immunopathogenesis and virus-host interactions of enterovirus 71 in patients with hand, foot and mouth disease. Front Microbiol 2017;8:2249.
8. Lei X, Cui S, Zhao Z, Wang J. Etiology, pathogenesis, antivirals and vaccines of hand, foot, and mouth disease. Natl Sci Rev 2015;2:268-84.
9. Bello AM, Roshorm YM. Recent progress and advances towards developing enterovirus 71 vaccines for effective protection against human hand, foot and mouth disease (HFMD). Biologicals 2022;79:1-9.
10. Yi EJ, Shin YJ, Kim JH, Kim TG, Chang SY. Enterovirus 71 infection and vaccines. Clin Exp Vaccine Res 2017;6:4-14.
11. Lu IN, Farinelle S, Sausy A, Muller CP. Identification of a CD4 T-cell epitope in the hemagglutinin stalk domain of pandemic H1N1 influenza virus and its antigen-driven TCR usage signature in BALB/c mice. Cell Mol Immunol 2017;14: 511-20.
12. He R, Yang X, Liu C, et al. Efficient control of chronic LCMV infection by a CD4 T cell epitope-based heterologous prime-boost vaccination in a murine model. Cell Mol Immunol 2018;15:815-26.
13. Larsen MV, Lundegaard C, Lamberth K, Buus S, Lund O, Nielsen M. Large-scale validation of methods for cytotoxic T-lymphocyte epitope prediction. BMC Bioinformatics 2007;8:424.
14. Reynisson B, Alvarez B, Paul S, Peters B, Nielsen M. NetMHCpan-4.1 and NetMHCIIpan-4.0: improved predictions of MHC antigen presentation by concurrent motif deconvolution and integration of MS MHC eluted ligand data. Nucleic Acids Res 2020;48:W449-54.
15. Saha S, Raghava GP. Prediction methods for B-cell epitopes. Methods Mol Biol 2007;409:387-94.
16. Dimitrov I, Bangov I, Flower DR, Doytchinova I. AllerTOP v.2: a server for in silico prediction of allergens. J Mol Model 2014;20:2278.
17. Doytchinova IA, Flower DR. VaxiJen: a server for prediction of protective antigens, tumour antigens and subunit vaccines. BMC Bioinformatics 2007;8:4.
18. Cheng J, Randall AZ, Sweredoski MJ, Baldi P. SCRATCH: a protein structure and structural feature prediction server. Nucleic Acids Res 2005;33:W72-6.
19. Gupta S, Kapoor P, Chaudhary K, et al. In silico approach for predicting toxicity of peptides and proteins. PLoS One 2013;8:e73957.
20. Vita R, Mahajan S, Overton JA, et al. The Immune Epitope Database (IEDB): 2018 update. Nucleic Acids Res 2019; 47(D1):D339-43.
21. Bui HH, Sidney J, Dinh K, Southwood S, Newman MJ, Sette A. Predicting population coverage of T-cell epitope-based diagnostics and vaccines. BMC Bioinformatics 2006;7:153.
22. Gasteiger E, Hoogland C, Gattiker A, et al. Protein identification and analysis tools on the Expasy server. In: Walker JM, editor. The proteomics protocols handbook. New York (NY): Humana Press; 2005. p. 571-607.
23. McGuffin LJ, Bryson K, Jones DT. The PSIPRED protein structure prediction server. Bioinformatics 2000;16:404-5.
24. Lee GR, Won J, Heo L, Seok C. GalaxyRefine2: simultaneous refinement of inaccurate local regions and overall protein structure. Nucleic Acids Res 2019;47:W451-5.
25. Laskowski RA, MacArthur MW, Moss DS, Thornton JM. PROCHECK: a program to check the stereochemical quality of protein structures. J Appl Crystallogr 1993;26:283-91.
26. Craig DB, Dombkowski AA. Disulfide by Design 2.0: a web-based tool for disulfide engineering in proteins. BMC Bioinformatics 2013;14:346.
27. Kozakov D, Hall DR, Xia B, et al. The ClusPro web server for protein-protein docking. Nat Protoc 2017;12:255-78.
28. van der Sanden S, Koopmans M, Uslu G, van der Avoort H; Dutch Working Group for Clinical Virology. Epidemiology of enterovirus 71 in the Netherlands, 1963 to 2008. J Clin

Microbiol 2009;47:2826-33.
29. Rapin N, Lund O, Bernaschi M, Castiglione F. Computational immunology meets bioinformatics: the use of prediction tools for molecular binding in the simulation of the immune system. PLoS One 2010;5:e9862.
30. Arita M, Nagata N, Iwata N, et al. An attenuated strain of enterovirus 71 belonging to genotype a showed a broad spectrum of antigenicity with attenuated neurovirulence in cynomolgus monkeys. J Virol 2007;81:9386-95.
31. Ooi EE, Phoon MC, Ishak B, Chan SH. Seroepidemiology of human enterovirus 71, Singapore. Emerg Infect Dis 2002;8:995-7.
32. Van Tu P, Thao NT, Perera D, et al. Epidemiologic and virologic investigation of hand, foot, and mouth disease, southern Vietnam, 2005. Emerg Infect Dis 2007;13:1733-41.
33. Bible JM, Pantelidis P, Chan PK, Tong CY. Genetic evolution of enterovirus 71: epidemiological and pathological implications. Rev Med Virol 2007;17:371-9.
34. Chan YF, Sam IC, AbuBakar S. Phylogenetic designation of enterovirus 71 genotypes and subgenotypes using complete genome sequences. Infect Genet Evol 2010;10:404-12.
35. Wu SC, Liu CC, Lian WC. Optimization of microcarrier cell culture process for the inactivated enterovirus type 71 vaccine development. Vaccine 2004;22:3858-64.
36. Tung WS, Bakar SA, Sekawi Z, Rosli R. DNA vaccine constructs against enterovirus 71 elicit immune response in mice. Genet Vaccines Ther 2007;5:6.
37. Murray KA, Allen T, Loh E, Machalaba C, Daszak P. Emerging viral zoonoses from wildlife associated with animal-based food systems: risks and opportunities. In: Jay-Russell M, Doyle M, editors. Food safety risks from wildlife: challenges in agriculture, conservation, and public health. Cham: Springer; 2016. p. 31-57.
38. Ojha R, Nandani R, Prajapati VK. Contriving multiepitope subunit vaccine by exploiting structural and nonstructural viral proteins to prevent Epstein-Barr virus-associated malignancy. J Cell Physiol 2019;234:6437-48.
39. Sharma A, Sanduja P, Anand A, et al. Advanced strategies for development of vaccines against human bacterial pathogens. World J Microbiol Biotechnol 2021;37:67.
40. Moise L, Gutierrez A, Kibria F, et al. iVAX: an integrated toolkit for the selection and optimization of antigens and the design of epitope-driven vaccines. Hum Vaccin Immunother 2015;11:2312-21.